Available online at www.sciencedirect.com
ScienceDirect
Bioorganic & Medicinal Chemistry 14 (2006) 7520–7530
Bioorganic & Medicinal Chemistry

Amino- and glycoconjugates of pyrido[4,3,2-*kl*]acridine. Synthesis, antitumor activity, and DNA binding

Laurent Bouffier,[a] Brigitte Baldeyrou,[b] Marie-Paule Hildebrand,[b] Amélie Lansiaux,[b] Marie-Hélène David-Cordonnier,[b] Danièle Carrez,[c] Alain Croisy,[c] Olivier Renaudet,[a] Pascal Dumy[a] and Martine Demeunynck[a,*]

[a]*LEDSS UMR5616 & ICMG-FR2607, Université Joseph Fourier, BP53, 38041 Grenoble cedex 9, France*
[b]*Inserm U814 and Laboratoire de Pharmacologie antitumorale, Centre Oscar Lambret, Institut de Recherches sur le Cancer de Lille, 1 place de Verdun 59045 Lille cedex, France*
[c]*INSERM U579, Centre Universitaire, 91405 Orsay and Institut Curie Recherche, Laboratoire Raymond Latarjet, France*

Received 17 May 2006; revised 21 June 2006; accepted 3 July 2006
Available online 1 August 2006

Abstract—A series of amino- and glycoconjugates of pyrido[4,3,2-*kl*]acridine and pyrido[4,3,2-*kl*]acridin-4-one have been prepared. The most active molecules, the amino conjugates **7** and **11**, display a cytostatic activity against HT-29 cancer cells at micromolar concentration. This activity correlates well with a strong DNA binding. The molecules, amino or glycoconjugates, bind DNA by intercalation, the amino or glyco substituent being located in one groove. None of the molecules inhibits topoisomerase activity.

1. Introduction

Pyrido[2,3,4-*kl*]acridines constitute a large class of cytotoxic agents from natural sources.[1–4] More than a hundred of molecules have been described, displaying a large variety of structural features. Due to their planar structure, their cytotoxicity has been related to their ability to bind DNA by intercalation but other biological activities have been highlighted such as topoisomerase inhibition,[5] production of reactive oxygen species, or release of calcium[4]. Stevens has described the synthesis of the isomeric pyrido[4,3,2-*kl*]acridine and evidenced a strong interaction with telomeric DNA that may be related to antitumor activities.[6] We have previously described the synthesis and chemical reactivity of pyrido[4,3,2-*kl*]acridine and pyrido[4,3,2-*kl*]acridin-4-one.[7,8] In particular, we have prepared a series of amino, polyamino, and thio substituted derivatives. In an effort to increase the structural diversity of the molecules, the introduction of sugars onto the pyridoacridine nucleus appears very attractive because glycoconjugates of planar polycycles such as anthracyclines,[9] rebeccamycin,[10] and related indolocarbazoles, or nogalamycin,[11] constitute a large class of DNA binding antitumor agents. The presence of the sugar moiety will also increase the solubility in water of the pyridoacridine nucleus and may possibly play a role in groove DNA binding. We report here the synthesis, cytotoxicity, and DNA binding of amino- and glycoconjugates of these two heterocycles.

2. Synthesis

The glycoconjugates **4a–d** were prepared as reported in Scheme 1 by formation of a chemoselective oxime bond between the formyl derivative **2** and the aminooxy sugars **3a–d**.[12] The formyl key-intermediate **2** was itself prepared as previously described.[7] Oxidative cleavage of the methoxy group by CAN afforded the corresponding pyridoacridin-4-one glycoconjugates **5a–d**. To prepare the amino conjugates **7–13**, we took advantage of the regioselective addition of amines to the pyridoacridone **6** itself prepared by CAN oxidation of **1** as previously published.[7]

Keywords: Acridine; Antitumor; DNA binding; Cytotoxicity; Pyridoacridine.
* Corresponding author. Tel.: +33 476 514429; fax: +33 476 514946; e-mail: martine.demeunynck@ujf-grenoble.fr

0968-0896/$ - see front matter © 2006 Elsevier Ltd. All rights reserved.
doi:10.1016/j.bmc.2006.07.010

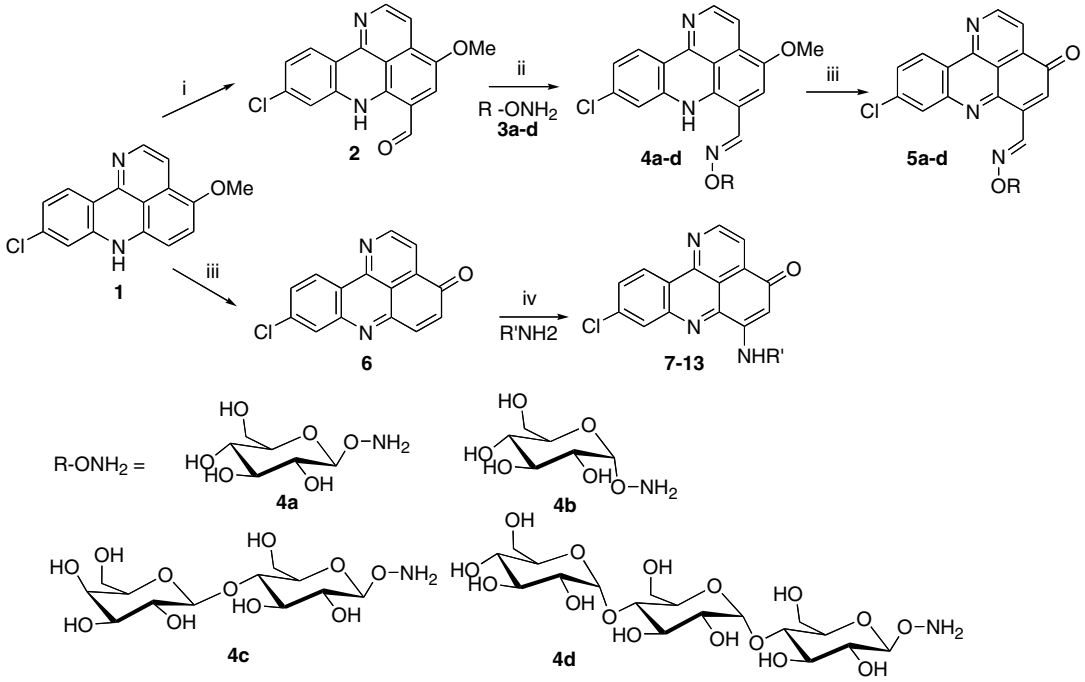

Scheme 1. Reagents and conditions: (i) DMF–$POCl_3$, CH_2Cl_2; (ii) $RONH_2$, MeOH, aq HCl, pH 4, 70 °C; (iii) CAN, CH_3CN–H_2O; (iv) $R'NH_2$ in large excess, EtOH–H_2O, 60 °C.

3. Results and discussion

3.1. In vitro antitumor activity

The conjugates were tested against HT29 tumor cells. The results, expressed as IC_{50}, are collected in Table 1.

The glycoconjugates **4a**–**d** and **5a**–**d** were found to be not cytotoxic ($IC_{50} > 50$ μM). This lack of cytotoxicity is independent of the nature of the heterocycle, that is, pyridoacridines (**4a**–**d**) or pyridoacridones (**5a**–**d**), and is not related to the presence of the sugar residue as the methoxy analogue (entry 5) is also devoid of cytotoxicity. The amino conjugates **7**–**13** show a significant cytostatic activity, the most active compounds (**7** and **11**) are active at micromolar concentration. The activity is related to the presence of at least one aliphatic amino group in the substituent (compare entries 10 with 15 or 16), compound with a tertiary amine being slightly more active than compound with a primary amine (compare entries 11 and 12). The length of the polymethylene linker separating the amino functions has a major influence on the activity, increasing the length of the linker decreases the activity (compare entries 10 and 11 or 12 and 13).

3.2. DNA binding properties

We measured the ability of selected conjugates to interact with DNA using several spectroscopic and biochemical approaches, the first one being absorption spectroscopy. As a result, addition of DNA induced a marked change in the absorption spectrum of each compound (Fig. 1) as revealed by both hypochromic and hypsochromic effects for compound **8** (Fig. 1A) or both hypochromic and bathochromic spectral modifications for the other derivatives (Fig. 1B–F). These DNA induced spectral changes reveal interesting interaction of the conjugates with the DNA helix.

As a second approach, we measured the ability of various concentrations of the chosen molecules to interfere with the thermal stability of double-stranded DNA (Fig. 2). Using both CT-DNA and polyd$(AT)_2$ oligonucleotides, the melting temperature (T_m) of DNA in the presence of each compound is shifted to higher temperature by comparison to that obtained without drug. However, the level of increased melting temperature (ΔT_m) induced by any of the six tested compounds is not in the same order of magnitude. Indeed, using CT-DNA (Fig. 2A and B) at increasing drug/DNA ratio reveals stronger ΔT_m values in the presence of **11** (up to +25.2 °C for a drug/DNA ratio of 0.5, Fig. 2B) than of **8**, **7**, and **10** (16.9, 13.3, and 12.2 °C, respectively, for drug/DNA ratio = 0.5), whereas a much smaller ΔT_m value is induced using the ribose-containing derivatives **4a** and **4b**. The same comparison in the efficiency of DNA helix stabilization by the drugs was observed using polyd$(AT)_2$ (Fig. 2C and D) but with higher values (up to 43 °C using **11** at a drug/DNA ratio = 0.5). Interestingly, two ΔT_m values were deduced from first derivative plots of the absorption spectra measured using either **11** or **8** at intermediate drug/DNA ratios as represented in the graph by the two ordinate values for the same abscissa value (Fig. 2D). The absorption spectra of thermal denaturation of polyd$(AT)_2$ in the presence of increased concentrations of **11** clearly reveal a two-transition curve (Fig. 2F), whereas a single transition was obtained using increasing concentrations of **7** (Fig. 2E).

Table 1. In vitro cytostatic activity against HT29 cell lines expressed in μM

Entry	Compound	R	IC_{50}
		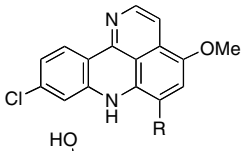	
1	**4a**	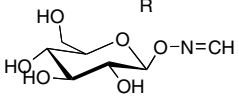	>50
2	**4b**	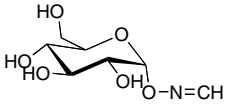	85
3	**4c**	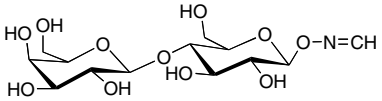	>50
4	**4d**	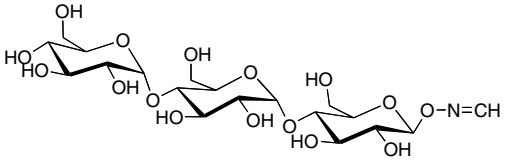	>50
5		CH=NOMe[a]	>50
		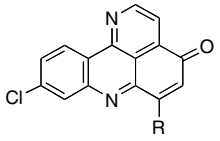	
6	**5a**	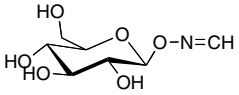	128
7	**5b**	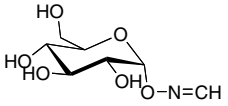	>50
8	**5c**	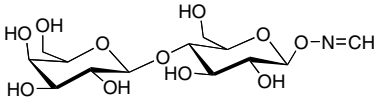	>50
9	**5d**	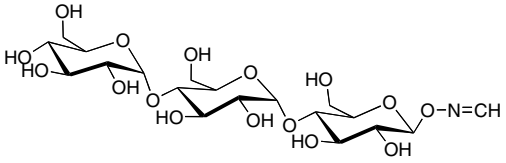	>50
10	**7**	$NH–(CH_2)_2–NMe_2$	1.8
11	**8**	$NH–(CH_2)_3–NMe_2$[a]	3
12	**9**	$NH–(CH_2)_3–NH_2$	4.7
13	**10**	$NH–(CH_2)_8–NH_2$	21
14	**11**	$NH–(CH_2)_3–NH–(CH_2)_3–NH_2$[a]	1.9
15	**12**	$NH–(CH_2)_2–OH$	16.5
16	**13**	$NH–C_6H_5$[b]	>100

[a] Ref. 7.
[b] Ref. 8.

Circular dichroism experiments were performed to investigate the mode of binding of the conjugates to DNA. No change in the CD spectra was observed using either **7**, **8**, **10** or **11**, whereas a positively induced CD is identified using **4a** and **4b** (Fig. 3). No CD could be seen using either **4a** or **4b** alone but a nice positively induced CD appears at 310 nm using both compounds in the presence of increasing concentrations of CT-

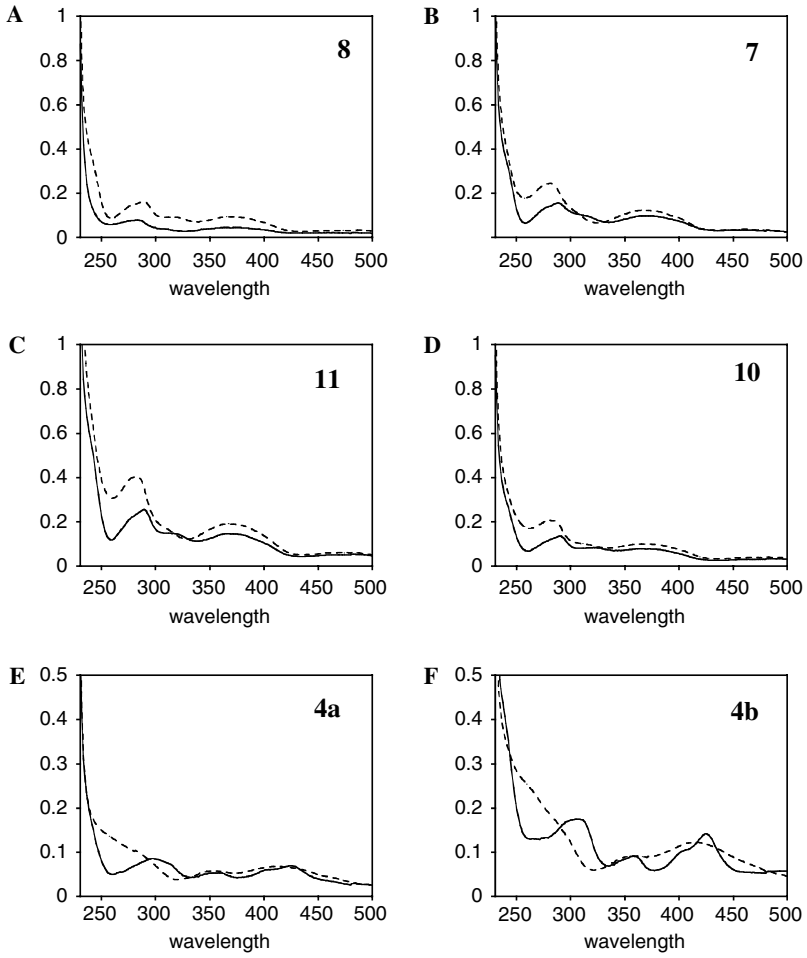

Figure 1. DNA binding of selected conjugates. Absorption spectra measurements of the tested compounds (20 μM) were obtained in the presence (solid lane) or absence (dashed lane) of CT-DNA (phosphate/DNA ratio $P/D = 20$) from 230 to 500 nm in BPE buffer. Spectra for amino conjugates (**8**,**7**,**11**, and **10**) are shown in A–D, and spectra for glycoconjugates **4a** and **4b** in E and F.

DNA. Another positively induced CD also appears at 400–430 nm using **4b** in accordance with the corresponding UV spectrum (Fig. 1F).

These results suggest that both glycoconjugates **4a** and **4b** interact with DNA by positioning the structure in one of the grooves of the helix, whereas the DNA binding mode of the other amino conjugates is much more complex and/or cannot be defined using CD experiments. In order to get an insight into the mode of binding by another complementary approach, topoisomerase I induced DNA relaxation assays were undertaken. Increasing concentrations of each of the derivatives were incubated with supercoiled plasmid DNA and treated with topoisomerase I. Separation of the various forms of plasmid DNA on an agarose gel stained post-electrophoresis using ethidium bromide reveals that any of the tested drugs interacts with DNA as typical intercalators (Fig. 4). Moreover, a nice gel shift of plasmid DNA is observed using **11**, and to a lesser extent using **7** and **8**, in accordance with the efficient binding activity of these compounds evidenced in melting temperature studies (Fig. 2).

In order to identify potential specific DNA binding sites of the various conjugates, DNase I footprinting experiments were undertaken (Fig. 5). Three different 3′-end labeled DNA fragments were incubated with increasing concentrations of the tested compounds. Neither **10**, **4a** nor **4b** reveals footprint using the 265 bp (Fig. 5A), 117 bp (data not shown) and 176 bp (Fig. 5B) DNA fragments. The decrease in the DNA ladder intensity seen in lanes for which the largest amounts of **7**, **8**, **10**, and **11** were used reveals non-specific DNA binding in agreement with the intercalative mode of binding of those derivatives. A relative low DNA sequence specificity (black boxes) could be deduced from DNase I cleavage of the DNA in the presence of smaller amount of compounds. No footprint can be seen on AT-rich stretches suggesting that those compounds do not bind through the minor groove of the DNA helix via AT-rich sequences as does the well-known minor groove binder netropsin (data not shown).

In a view to address the biological action of the various conjugates, they were tested for their ability to poison either topoisomerase I or II. Figure 6 reveals that no stable topoI–conjugate–DNA complexes were formed on agarose gel suggesting the lack of direct effect of conjugates on the topoisomerase I enzyme. However, a strong DNA binding is observed on supercoiled DNA reinforcing

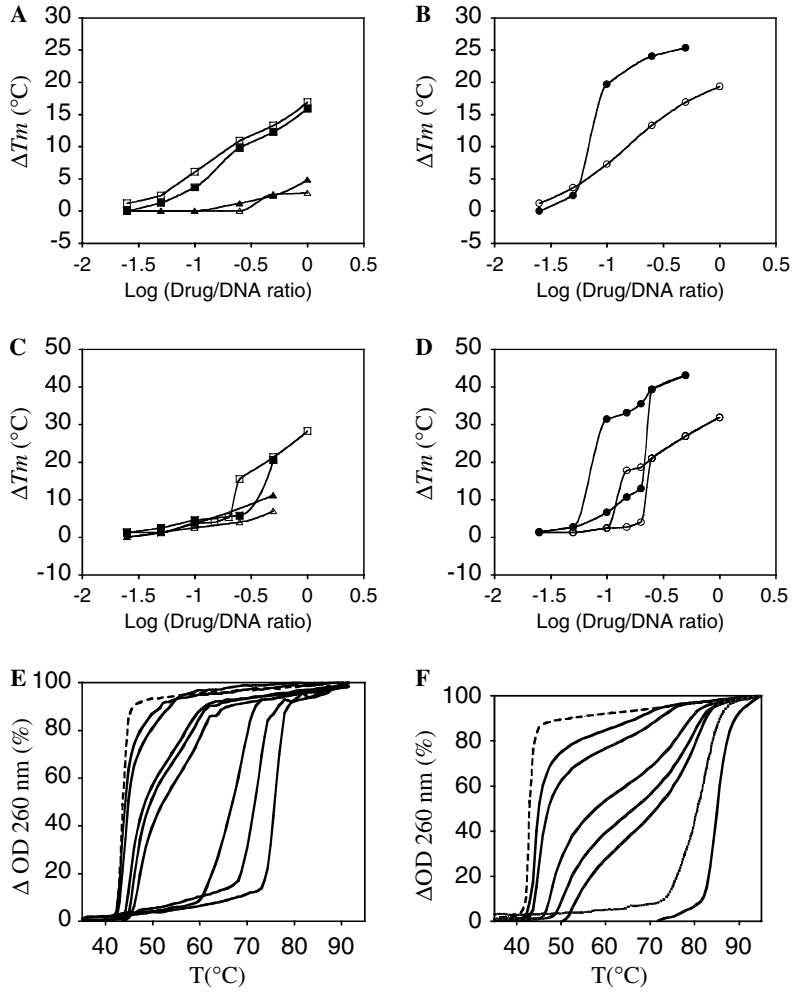

Figure 2. Melting temperature studies. The variations of the melting temperature of CT-DNA (A–B) or poly(dAT)$_2$ (C–D) were measured in BPE buffer by incubating 20 μM DNA (base pairs) alone or with increasing concentrations of compounds **4a** (Δ), **4b** (▲), **7** (□), **8** (○), **10** (■) or **11** (●) in order to obtain phosphate/DNA ratios from 0.025 to 1. The graphs are expressed as T_m (drug + DNA) − T_m (DNA alone) over the log10 of the drug/base pair ratio. The various spectra for measurement of the melting of poly(dAT)$_2$ by increasing concentrations of **7** or **11** are presented in (E) and (F), respectively, and are expressed as the percentage of increase of the absorbency at 260 nm over the increase of temperature.

the previous observation that **11** was the most efficient DNA binding derivative (Fig. 2). No activity on topoisomerase II was observed (data not shown).

4. Conclusion

We have prepared a series of glyco- and amino conjugates derived from pyrido[4,3,2-*kl*]acridine and pyrido[4,3,2-*kl*]acridin-4-one as potential antitumor agents. The molecules were tested against HT-29 cancer cells. The glycoconjugates are not cytotoxic compared to the amino conjugates that show cytostatic activity at micromolar concentration. This cytostatic effect correlates well with DNA binding potency, the most cytostatic molecules **7** and **11** displaying the strongest DNA binding as shown by melting temperature experiments. The molecules bind to DNA by intercalation. This binding is reinforced by the presence of protonated aliphatic amino groups that can interact with the phosphate backbone of the macromolecule. It should be noted that unlike what was generally observed for acridine or pyridoacridine alkaloids, no inhibition of topoisomerase activity was found.

5. Experimental

^{1}H nuclear magnetic resonance (NMR) spectra were recorded at 200 or 300 MHz, either in chloroform-*d* ($CDCl_3$) with residual $CHCl_3$ (δ = 7.26 ppm), dimethyl-d_6 sulfoxide (DMSO-d_6) with residual peak (δ = 2.50 ppm) or methanol-d_4 (CD_3OD) with residual CH_3OD (δ = 3.31 ppm) as internal standard, at room temperatures (298 K). The direct chemical ionization (DCI) mass spectra were obtained on a Thermo Filligan PolarisQ with NH_3/isobutane as the reagent gas. The electron spray ionization mass spectrometry (ESI-MS) was recorded on a VG Platform II (Micromass). Reverse-phase HPLC analyses were performed on Waters equipment consisting of a Waters 600 controller and a Waters 2487 dual absorbance detector. The preparative column (Delta-Pak 300 Å 15 μm C_{18} particles, 200 × 25 mm^2) was operated at 22 mL/min, with UV monitoring at 214

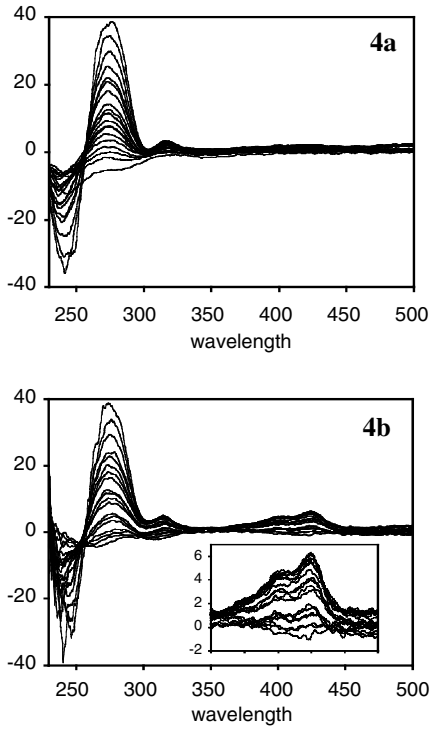

Figure 3. Circular dichroism measurements. CD titrations were performed with 50 μM of **4a** and **4b** incubated with graded concentrations of CT-DNA from *P*/*D* ratio = 0.4 to 14. The portion of graph B corresponding to the wavelength from 350 to 475 nm was amplified and is presented just below the corresponding portion of the CD titration graph.

and 450 nm. Solvent B consisted of 0.1% TFA in 90% acetonitrile, and solvent A, of 0.1% TFA.

Compounds **8**, **11**, and **13** have already been described.[7]

5.1. General Procedure for drug–sugar conjugation

5.1.1. 9-Chloro-4-methoxy-6-(β-D-glucopyranosyliminomethylene)-7*H*-pyrido[4,3,2-*kl*]acridine (4a). To a mixture of the aldehyde **2** (0.0252 g, 0.081 mmol) and β-D-glucopyranosyl-oxyamine **3a** (0.0179 g, 0.092 mmol) in anhydrous MeOH (4 mL), 10 μL MeOH/HCl(g) was added in order to adjust the pH value at pH 4. The solution was refluxed for 19 h. The solvent was then evaporated under vacuum and the crude product purified by preparative HPLC. Conjugate **4a** was obtained after lyophilization in 32% yield (0.0134 g, 0.028 mmol). ^{1}H NMR (300 MHz, DMSO-d_6): δ 11.10 (1H, s, NH); 8.78 (1H, s, ArCHN); 8.29 (1H, d, J = 8.7 Hz, H-11); 8.33 (1H, d, J = 6.1 Hz, H-2); 7.60 (1H, s, H-8); 7.54 (1H, s, H-5); 7.50 (1H, d, J = 6.1 Hz, H-3); 7.28 (1H, d, J = 8.7 Hz, H-10); 5.23 (1H, d, J = 8.0 Hz); 3.96 (3H, s, Me); 3.75 (1H, d, J = 11.5 Hz); 3.55–3.15 (5H, m). MS (ESI): m/z = 488.1 (M+H)$^+$.

5.1.2. 9-Chloro-4-methoxy-6-(α-D-glucopyranosyliminomethylene)-7*H*-pyrido[4,3,2-*kl*]acridine (4b). Following the previous procedure, starting from **2** (0.0218 g, 0.070 mmol) and α-D-glucopyranosyl-oxyamine **3b** (0.0157 g, 0.081 mmol), the reaction mixture was stirred for 23 h and compound **4b** was obtained in 94% yield (0.0321 g, 0.066 mmol). ^{1}H NMR (300 MHz, DMSO-d_6): δ 11.10 (1H, s, NH); 8.80 (1H, s, ArCHN); 8.44 (1H, d, J = 8.7 Hz, H-11); 8.28 (1H, d, J = 6.1 Hz, H-2); 7.66 (1H, s, H-8); 7.54 (1H, s, H-5); 7.47 (1H, d, J = 6.1 Hz, H-3); 7.25 (1H, d, J = 8.7 Hz, H-10); 5.81 (1H, d, J = 8.0 Hz); 3.94 (3H, s, Me); 3.65–3.17 (6H, m). MS (ESI): m/z = 488.1 (M+H)$^+$.

5.1.3. 9-Chloro-4-methoxy-6-(β-D-lactosyliminomethylene)-7*H*-pyrido[4,3,2-*kl*]acridine (4c). Following the

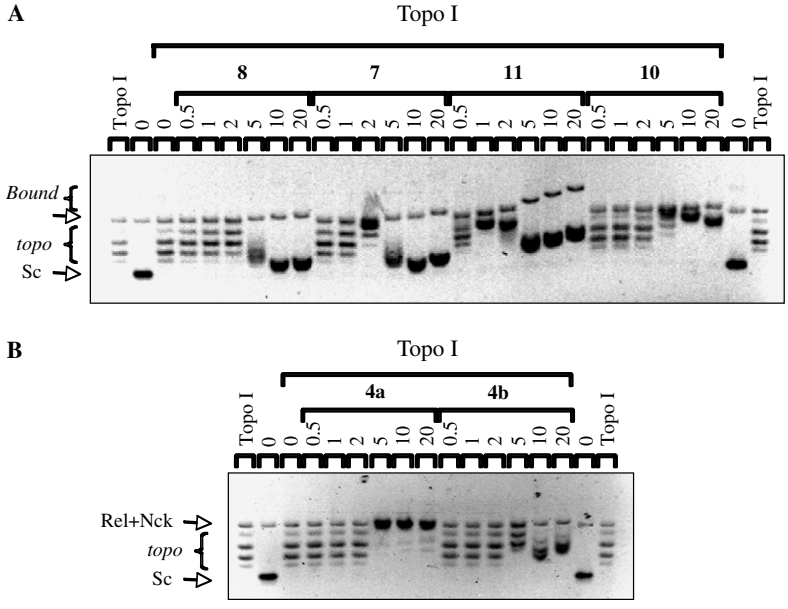

Figure 4. Relaxation of DNA mediated by topoisomerase I. Native supercoiled pLAZ plasmid (0.13 μg, lanes 0) was incubated with 4 U of topoisomerase I in the absence (lanes Topo I) or presence of increasing concentrations of the tested compounds at the indicated concentrations (μM). The DNA samples were treated as described in Materials and methods and separated by electrophoresis on a 1% agarose gel which was stained with ethidium bromide after migration of the DNA. Sc and Rel correspond to the supercoiled and relaxed forms of the plasmid DNA, whereas *topo* and *Bound* refer to the topoisomer products and the gel shifted drug-relaxed DNA complex, respectively. Data for amino conjugates (**8**,**7**,**11**, and **10**) are shown in A, and data for glycoconjugates **4a** and **4b** in B.

previous procedure, starting from **2** (0.0143 g, 0.046 mmol) and β-D-lactosyl-oxyamine **3c** (0.0187 g, 0.052 mmol), the reaction mixture was stirred for 25 h and compound **4c** was obtained in 66% yield (0.0221 g, 0.030 mmol). ^{1}H NMR (300 MHz, DMSO-d_6): δ 11.01 (1H, s, NH); 8.79 (1H, s, ArCHN); 8.43 (1H, d, J = 8.7 Hz, H-11); 8.37 (1H, d, J = 6.0 Hz, H-2); 7.60 (1H, d, J = 2.0 Hz, H-8); 7.51 (1H, d, J = 6.0 Hz, H-3); 7.50 (1H, s, H-5); 7.26 (1H, dd, J = 8.7 and 2.0 Hz, H-10); 5.32 (1H, d, J = 8.0 Hz); 4.26 (1H, d, J = 6.8 Hz); 3.95 (3H, s, Me); 3.82–3.20 (12H, m). MS (ESI): m/z = 650.2 $(M+H)^+$.

5.1.4. 9-Chloro-4-methoxy-6-(β-D-maltotriosyliminomethylene)-7*H*-pyrido[4,3,2-*kl*]acridine (4d). Following the previous procedure, starting from **2** (0.0140 g, 0.045 mmol) and β-D-maltotriosyl-oxyamine **3d** (0.0270 g, 0.052 mmol), the reaction mixture was stirred for 19 h and compound **4d** was obtained in 53% yield (0.0235 g, 0.024 mmol). ^{1}H NMR (300 MHz, DMSO-d_6): δ 10.94 (1H, s, NH); 8.78 (1H, s, ArCHN); 8.44 (1H, d, J = 8.7 Hz, H-11); 8.40 (1H, d, J = 5.9 Hz, H-2); 7.57 (1H, d, J = 1.8 Hz, H-8); 7.50 (1H, d, J = 5.9 Hz, H-3); 7.46 (1H, s, H-5); 7.24 (1H, dd, J = 8.7 and 1.8 Hz, H-10); 5.27 (1H, d, J = 8.2 Hz); 5.09 (1H, d, J = 4.0 Hz); 5.01 (1H, d, J = 3.7 Hz) 3.95 (3H, s, Me); 3.77–3.04 (18H, m). MS (ESI): m/z = 812.2 $(M+H)^+$.

5.2. General procedure for drug–sugar conjugates' oxidative demethylation

5.2.1. 9-Chloro-6-(β-D-glucopyranosyliminomethylene)-4*H*-pyrido[4,3,2-*kl*]acridin-4-one (5a). To conjugate **4a** (0.0045 g, 0.0092 mmol) dissolved in a 2/1 acetonitrile/water mixture (4.5 mL) was added CAN (0.020 g, 0.037 mmol). The solution was stirred at room temperature for 15 min and then kept for 1 h at 2–4 °C. The suspension was collected by filtration, washed with Et_2O, and the product **5a** was obtained in 78% yield (0.0034 g, 0.0072 mmol). ^{1}H NMR (300 MHz, DMSO-d_6): δ 9.57 (1H, d, J = 4.6 Hz, H-2); 9.12 (1H, s, ArCHN); 9.09 (1H, d, J = 8.7 Hz, H-11); 8.44 (1H, d, J = 2.0 Hz, H-8); 8.25 (1H, d, J = 4.6 Hz, H-3); 8.00 (1H, dd, J = 8.7 and

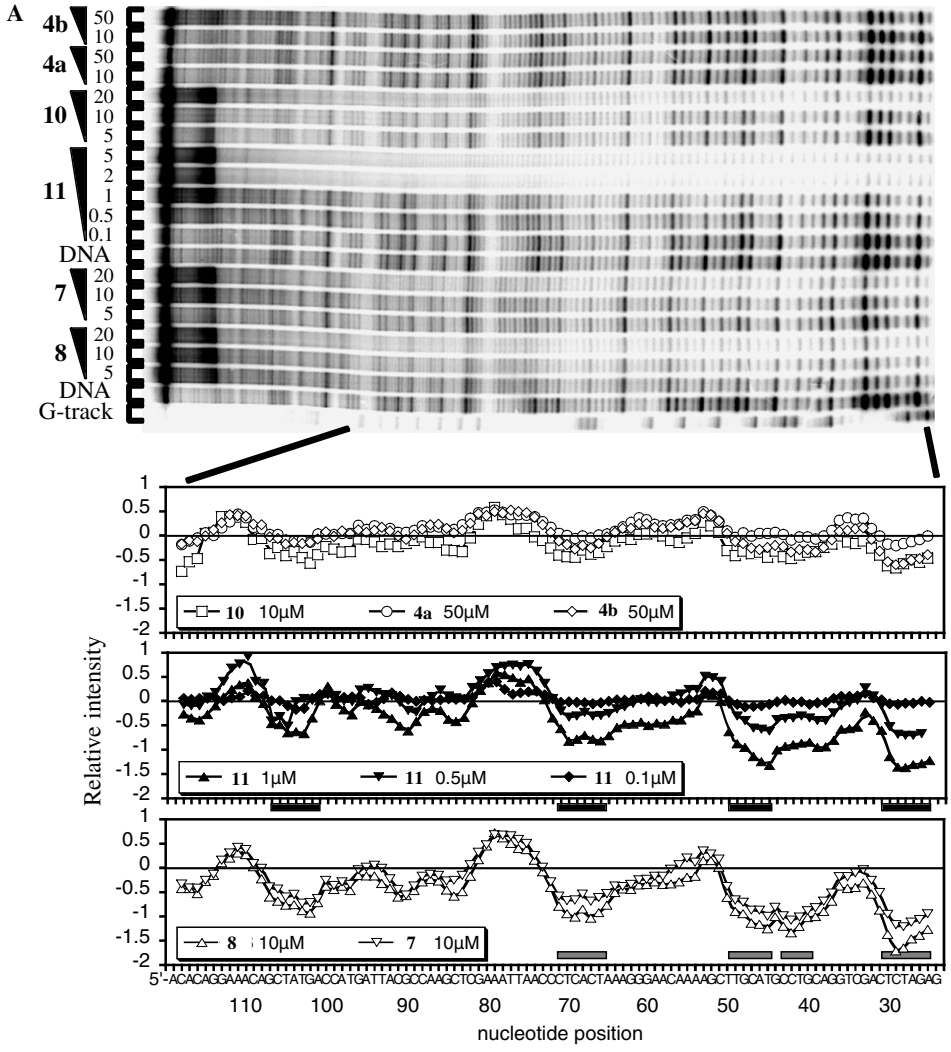

Figure 5. (A/B) DNase I footprinting experiments. Increasing concentrations (indicated on the left of each lane, μM) of the tested derivatives were incubated with the 265 bp (A) or 176 bp (B) 3′-end labeled DNA fragments prior to be subjected to DNase I soft digestion. After separation on a 8% polyacrylamide denaturing gel, the resulting digested DNA fragments were quantified and compared with the control lane containing no drug (DNA) to obtain the densitometric analysis. The G-track lane was used as a marker of the DNA sequence. Gray boxes refer to DNase I footprints obtained using either **7** or **8** compounds, whereas the black boxes reveal the relevant footprints obtained in the presence of increasing concentrations of **11**.

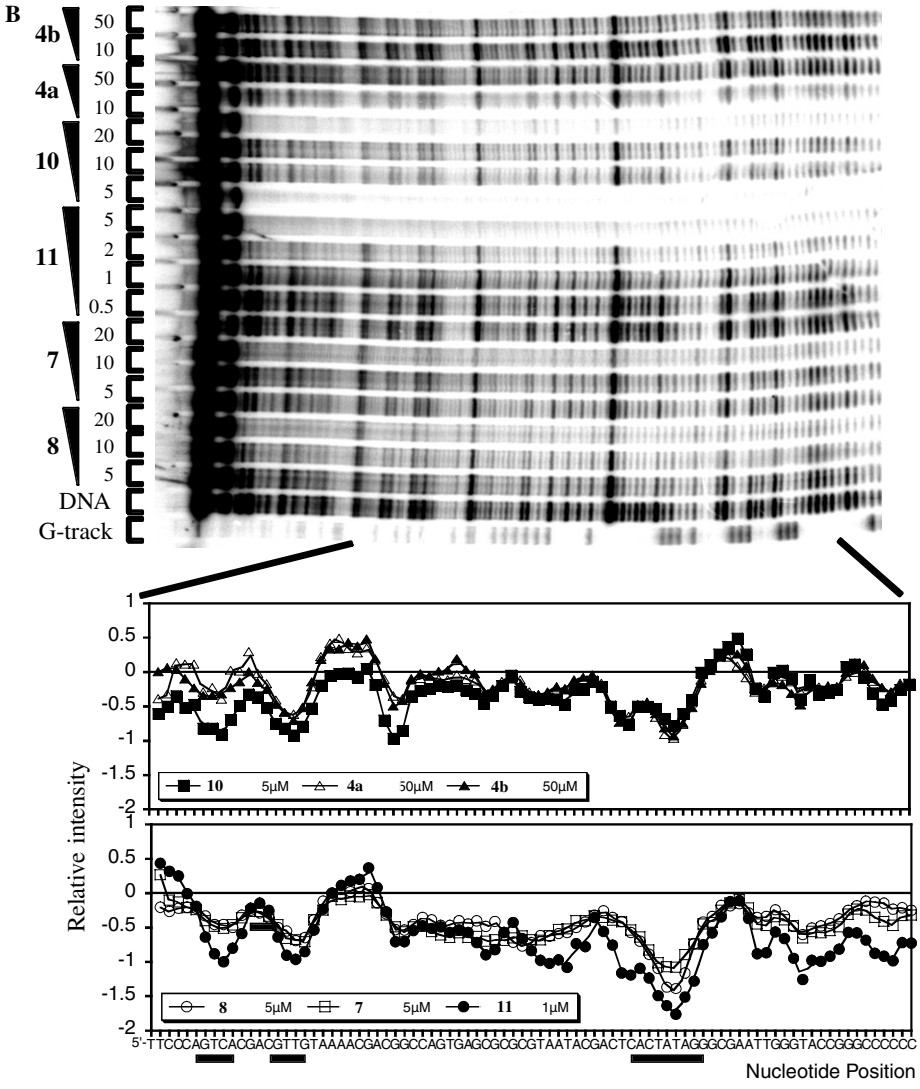

Figure 5 (*continued*)

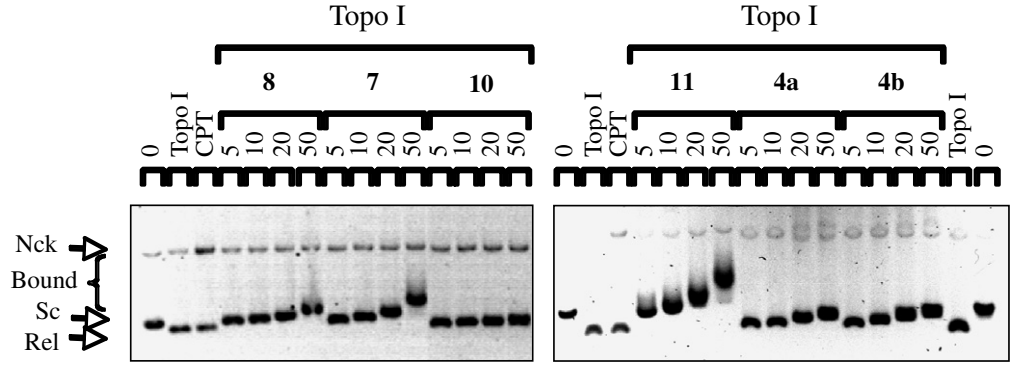

Figure 6. Inhibition of DNA religation by topoisomerase I. Native supercoiled pLAZ plasmid (0.13 μg, lanes 0) was incubated with topoisomerase I in the absence (lane Topo I) or presence of tested compounds from 5 to 50 μM. The DNA samples were separated by electrophoresis on a 1% agarose gel containing ethidium bromide. Sc, Rel, Nck, and Lin refer to the supercoiled, relaxed, open circular, and linearized forms of the plasmid DNA, respectively. Bound corresponds to shifted DNA due to gel retardation of the plasmid DNA by strong binding of tested compounds.

2.0 Hz, H-10); 7.28 (1H, s, H-5); 5.07 (1H, d, J = 8.1 Hz); 3.73–3.17 (6H, m). MS (ESI): m/z = 472.0 $(M+H)^+$.

5.2.2. 9-Chloro-6-(α-D-glucopyranosyliminomethylene)-4*H*-pyrido[4,3,2-*kl*]acridin-4-one (5b). Following the previous procedure, starting from **4b** (0.0075 g, 0.0153 mmol) and CAN (0.034 g, 0.062 mmol), **5b** was obtained in 83% yield (0.006 g, 0.0127 mmol). ^{1}H NMR (300 MHz, DMSO-d_6): δ 9.55 (1H, d, J = 4.6 Hz, H-2); 9.12 (1H, s, ArCHN); 9.04 (1H, d, J = 8.8 Hz, H-11); 8.43 (1H, d, J = 1.9 Hz, H-8); 8.23 (1H, d, J = 4.6 Hz, H-3); 7.98 (1H, dd, J = 8.8 and

1.9 Hz, H-10); 7.27 (1H, s, H-5); 5.56 (1H, d, $J = 3.7$ Hz); 3.64–3.19 (6H, m). MS (ESI): $m/z = 471.9$ $(M+H)^+$.

5.2.3. 9-Chloro-6-(β-D-lactosyliminomethylene)-4*H*-pyrido[4,3,2-*kl*]acridin-4-one (5c). Following the previous procedure, starting from **4c** (0.0075 g, 0.0152 mmol) and CAN (0.036 g, 0.066 mmol), **5c** was obtained in 80% yield (0.0077 g, 0.0122 mmol). ^{1}H NMR (300 MHz, DMSO-d_6): δ 9.56 (1H, d, $J = 4.6$ Hz, H-2); 9.12 (1H, s, ArCHN); 9.07 (1H, d, $J = 8.8$ Hz, H-11); 8.43 (1H, d, $J = 2.0$ Hz, H-8); 8.24 (1H, d, $J = 4.6$ Hz, H-3); 7.99 (1H, dd, $J = 8.8$ and 2.0 Hz, H-10); 7.27 (1H, s, H-5); 5.17 (1H, d, $J = 8.2$ Hz); 4.25 (1H, d, $J = 7.1$ Hz); 3.79–3.33 (14H, m). MS (ESI): $m/z = 634.0$ $(M+H)^+$.

5.2.4. 9-Chloro-6-(β-D-maltotriosyliminomethylene)-4*H*-pyrido[4,3,2-*kl*]acridin-4-one (5d). Following the previous procedure, starting from **4d** (0.0125 g, 0.0154 mmol) and CAN (0.034 g, 0.062 mmol), **5d** was obtained in 57% yield (0.007 g, 0.0088 mmol). ^{1}H NMR (300 MHz, DMSO-d_6): δ 9.57 (1H, d, $J = 4.6$ Hz, H-2); 9.12 (1H, s, ArCHN); 9.08 (1H, d, $J = 8.7$ Hz, H-11); 8.43 (1H, d, $J = 1.9$ Hz, H-8); 8.25 (1H, d, $J = 4.6$ Hz, H-3); 8.00 (1H, dd, $J = 8.7$ and 1.9 Hz, H-10); 7.28 (1H, s, H-5); 5.13 (1H, d, $J = 8.2$ Hz); 5.08 (1H, d, $J = 3.7$ Hz); 5.01 (1H, d, $J = 3.7$ Hz); 3.74–3.07 (18H, m). MS (ESI): $m/z = 796.1$ $(M+H)^+$.

5.3. General procedure for drug–amine conjugation

5.3.1. 9-Chloro-6-(2-(dimethylamino)-1-ethylamino)-4*H*-pyrido[4,3,2-*kl*]acridin-4-one (7). To a solution of compound **6** (0.098 g, 0.367 mmol) in 42 mL EtOH/H_2O (4/1) mixture was added an excess of 2-(dimethylamino)-1-ethylamine (1.90 mL, 18.35 mmol). The solution was stirred at 60 °C for 1 h. The solution was then acidified by addition of 11 N HCl and washed twice with CH_2Cl_2. The aqueous layer was neutralized by adding aqueous NaOH and extracted with dichloromethane. The organic layer was dried over sodium sulfate and evaporated under vacuum. Compound **7** was obtained in 77% yield (0.100 g, 0.282 mmol). Mp 213–216 °C. ^{1}H NMR (200 MHz, $CDCl_3$): δ 9.24 (1H, d, $J = 4.5$ Hz, H-2); 8.95 (1H, d, $J = 8.8$ Hz, H-11); 8.18 (1H, d, $J = 2.0$ Hz, H-8); 8.10 (1H, d, $J = 4.5$ Hz, H-3); 7.69 (1H, dd, $J = 8.8$ and 2.0 Hz, H-7); 7.65 (1H, t, NH); 5.82 (1H, s, H-5); 3.44 (2H, q, $J = 5.8$ Hz, NH-CH_2); 2.76 (2H, t, $J = 6.1$ Hz, CH_2–NMe_2); 2.38 (6H, s, 2 Me). MS (DCI): $m/z = 353.2$ $(M+H)^+$.

5.3.2. 9-Chloro-6-(3-(amino)-1-propylamino)-4*H*-pyrido[4,3,2-*kl*]acridin-4-one (9). Following the previous procedure, starting from **6** (0.100 g, 0.375 mmol) and 1,3-diaminopropane (1.70 mL, 18.75 mmol), after 3 h of reaction, compound **9** was isolated in 49% yield (0.061 g, 0.181 mmol). Mp 169–174 °C. ^{1}H NMR (300 MHz, $CDCl_3$): δ 9.33 (1H, d, $J = 4.6$ Hz, H-2); 9.06 (1 H, d, $J = 8.7$ Hz, H-11); 8.21–8.19 (2H, m, H-8 and H-3); 7.86 (1H, m, NH); 7.77 (1H, dd, $J = 8.7$ and 2.1 Hz, H-7); 5.93 (1H, s, H-5); 3.53 (2H, q, $J = 6.4$ Hz, NH–CH_2); 2.99 (2H, t, $J = 6.5$ Hz, CH_2–NH_2); 1.97 (2H, quint, $J = 6.7$ Hz, CH_2). MS (DCI): $m/z = 339.0$ $(M+H)^+$.

5.3.3. 9-Chloro-6-(8-(amino)-1-octylamino)-4*H*-pyrido[4,3,2-*kl*]acridin-4-one (10). Following the previous procedure, starting from **6** (0.100 g, 0.375 mmol) and 1,8-diaminooctane (2.50 mL, 18.75 mmol), after 1.5 h of reaction, compound **10** was isolated in 72% yield (0.110 g, 0.268 mmol). Mp 125–130 °C. ^{1}H NMR (300 MHz, CD_3OD): δ 9.17 (1 H, d, $J = 4.5$ Hz, H-2); 8.84 (1H, d, $J = 8.7$ Hz, H-11); 8.09 (1H, d, $J = 2.2$ Hz, H-8); 7.97 (1H, d, $J = 4.5$ Hz, H-3); 7.70 (1H, dd, $J = 8.8$ and 2.2 Hz, H-10); 5.73 (1H, s, H-5); 3.35 (2H, t, $J = 7.2$ Hz, CH_2); 2.56 (4H, dt, $J = 7.2$ and 1.8 Hz, 2 CH_2); 1.72 (2H, quint, $J = 7.2$ Hz, CH_2); 1.41–1.18 (10H, m, 5 CH_2). MS (DCI): $m/z = 409.2$ $(M+H)^+$.

5.3.4. 9-Chloro-6-(2-hydroxyethylamino)-4*H*-pyrido[4,3,2-*kl*]acridin-4-one (12). Following the previous procedure, starting from **6** (0.101 g, 0.375 mmol) and 2-aminoethanol (1.14 mL, 18.75 mmol), after 24 h of reaction, compound **12** was isolated in 25% yield (0.031 g, 0.095 mmol). Mp 232–236 °C. ^{1}H NMR (300 MHz, DMSO-d_6): δ 9.44 (1H, d, $J = 4.6$ Hz, H-2); 9.05 (1H, d, $J = 8.8$ Hz, H-11); 8.31 (1H, d, $J = 2.2$ Hz, H-8); 8.11 (1H, d, $J = 4.5$ Hz, H-3); 8.06 (1H, d, $J = 6{,}0$ Hz, NH); 7.97 (1H, dd, $J = 8.8$ and 2.2 Hz, H-10); 5.93 (1H, s, H-5); 5.02 (1H, t, $J = 5.5$ Hz, OH); 3.74 (2H, q, $J = 5.6$ Hz, CH_2–OH); 3.49 (2H, q, $J \approx 5.9$ Hz, CH_2–NH). MS (DCI): $m/z = 326.1$ $(M+H)^+$.

5.4. In vitro cytostatic activity

HT29 cells were cultivated in Dulbecco's MEM supplemented with 10% FCS. Cells from log-phase culture were seeded in 24-microwell plates (1 ml-5×10^{-4} cells/well) and incubated for two days. Tested compounds, in DMSO solution, were added under the minimum volume (5 μl) in increasing concentration. Control cells received 5 μl DMSO alone. Plates were incubated for 24 h, then medium was removed and cells washed twice with phosphate-buffered saline before addition of fresh medium free of drug. Plates were reincubated for three days before evaluation of the cell survival using the MTT assay using 30-min incubation with 100 μg/well of 3-[4,5-dimethylthiazol-2-yl]-2,5-diphenyl tetrazolium bromide (MTT, Sigma). After removal of the medium, formazan crystals were taken up with 100 μl DMSO and absorbance at 540 nm was measured with a microplate reader (Model 450 Bio-Rad), survival was expressed as % of DMSO treated controls. All incubations were carried out at 37 °C in a water-jacketed CO_2 incubator (5% CO_2, 100% relative humidity). Cytostatic activity was expressed as IC_{50}, the concentration that reduced by 50% the number of treated cells relative to controls. IC_{50} values were extracted from regression curves obtained with experimental points.

5.5. DNA binding

Double-stranded poly(dAT)$_2$ oligonucleotide and CT-DNA were obtained from Sigma. After dissolution, CT-DNA was deproteinized using sodium dodecyl sulfate and then dialyzed against 1 mM sodium cacodylate (pH 7.0). The concentrations of DNA were determined

from their molar extinction coefficients of 6600 M^{-1} cm^{-1}. Synthesized compounds, as well as camptothecin and etoposide (Sigma), were dissolved as 10 mM solutions in DMSO. Further dilutions were made in the appropriate aqueous buffer.

5.5.1. Absorption spectrometry and melting temperature studies. UV/visible spectra were measured using an Uvikon 943 spectrophotometer. Typically, 20 μM of the various drugs was prepared in 1 mL of BPE buffer [6 mM Na_2HPO_4, 2 mM NaH_2PO_4, and 1 mM EDTA, pH 7.1] in the presence or absence of 20 μM of base pairs of CT-DNA and transferred in a quartz cuvette of 10 mm pathlength. The spectra were recorded from 230 to 500 nm and are referenced against a cuvette containing the same DNA concentration in the same buffer. For the absorption titration, CT-DNA was added gradually from 1 to 20 μM with a spectrum recorded after each addition.

To perform the melting temperature measurement, 20 μM of CT-DNA or poly(dAT)2 was incubated alone (control T_m) or with increasing concentrations of the tested compounds in 1 mL of BPE buffer thus resulting in a drug/base pair ratio of 0.025, 0.05, 0.1, 0.15, 0.2, 0.25, 0.5 or 1. The samples were transferred in quartz cells and the absorbency at 260 nm was measured every min over the range of 20–100 °C with an increment of 1 °C per minute using the Uvikon 943 spectrophotometer thermostated with a Neslab RTE111 cryostat. The T_m values were obtained from the midpoint of the hyperchromic transition.

5.5.2. Circular dichroism. The CD spectra were obtained using a J-810 Jasco spectropolarimeter at 20 °C controlled by a PTC-424 S/L peltier type cell changer (Jasco). A quartz cell of 10 mm pathlength was used to obtain spectra from 500 to 230 nm with a resolution of 0.1 nm. The various drugs (50 μM final concentration) were incubated in 1 ml of sodium cacodylate (1 mM, pH 7.0) without (control) or with 200 μM (base pairs) of CT-DNA or increasing concentrations of CT-DNA (10, 20, 30, 40, 50, 60, 70, 80, 90, 100, 120, 140, 160, 180, and 200 μM).

5.5.3. Topoisomerase I-mediated DNA relaxation. Supercoiled pLAZ plasmid DNA (130 ng) was incubated with 4 U of human topoisomerase I (TopoGen) at 37 °C for 45 min in 20 μL of relaxation buffer (50 mM tris(hydroxymethyl) aminomethane (pH 7.8), 50 mM KCl, 10 mM $MgCl_2$, 1 mM dithiothreitol, 1 mM EDTA, and 1 mM ATP) in the presence of graded concentrations (from 0.5 to 20 μM) of the tested compounds. The reactions were terminated by addition of SDS to 0.25% and proteinase K to 250 μg/mL and incubation at 50 °C for a further 30 min. Three microlitres of the electrophoresis dye mixture was then added to DNA samples which were then separated by electrophoresis in a 1% agarose gel containing (topoisomerase DNA cleavage gel) or not (inhibition of the relaxation of DNA) ethidium bromide (1 μg/mL) at room temperature for 2 h at 120 V in TBE buffer (89 mM Tris base, 89 mM boric acid, and 2.5 mM Na_2EDTA, pH 8.3). Gels run without ethidium bromide were then stained using a bath containing ethidium bromide. Both gels were finally washed and photographed under UV light.

5.5.4. DNase I footprinting. A 265 bp 3′-end-labeled DNA fragment was obtained from double digestion of the pBS plasmid (Stratagene, La Jolla, CA) using *Eco*RI and *Pvu*II restriction enzymes for 1 h in their respective buffers followed by incubation with α-[^{32}P]dATP (Amersham, Buckinghamshire, England) and AMV reverse transcriptase for 2 h. The 265 bp radio-labelled DNA fragment was then separated on a 6% polyacrylamide gel under native conditions in TBE buffer, cut off from the gel, crushed, and dialyzed overnight against 400 μl of 10 mM Tris, pH 8.0, 1 mM EDTA, and 100 mM NaCl. After filtration under a 0.45 μm filter, the purified DNA was ethanol precipitated. Appropriate concentrations of the various ligands were incubated with the 265-bp radio-labeled DNA fragment for 15 min at 37 °C to ensure equilibrium prior to digestion of the DNA by the addition of DNase I (0.01 U/ml) in 20 mM NaCl, 2 mM $MgCl_2$, and 2 mM $MnCl_2$, pH 7.3. After 3 min, the reaction was stopped by freeze-drying and samples were lyophilized. The DNA samples were dissolved in 5 μL of denaturing loading buffer (80% formamide solution containing tracking dyes), heated at 90 °C for 4 min, and chilled in ice for 4 min prior to be loaded on a classical 8% denaturing polyacrylamide gel containing 8 M urea for 90 min at 65 W in TBE buffer. The data were collected using a Molecular Dynamics 445SI PhosphorImager and analyzed using the ImageQuant version 4.1 software. Each resolved band on the autoradiograph was assigned to a particular bond within the DNA fragment by comparison of its position relative to the guanines sequencing standard (G-track) classically obtained using DMS and piperidine treatment of the same DNA fragment.

Acknowledgments

This work was supported by grants from the Institut de Recherches sur le Cancer de Lille (IRCL) and from the MENRT (grant to L.B.).

References and notes

1. Marshall, K. M.; Barrows, L. R. *Nat. Prod. Rep.* **2004**, *21*, 731.
2. Ding, Q.; Chichak, K.; Lown, J. W. *Curr. Med. Chem.* **1999**, *6*, 1.
3. Delfourne, E.; Bastide, J. *Med. Res. Rev.* **2003**, *23*, 234.
4. Molinski, T. F. *Chem. Rev.* **1993**, *93*, 1825.
5. Dias, N.; Vezin, H.; Lansiaux, A.; Bailly, C. *Top. Curr. Chem.* **2005**, *253*, 89.
6. Heald, R. A.; Modi, C.; Cookson, J. C.; Hutchinson, I.; Laughton, C. A.; Gowan, S. M.; Kelland, L. R.; Stevens, M. F. G. *J. Med. Chem.* **2002**, *45*, 590.
7. Bouffier, L.; Demeunynck, M.; Milet, A.; Dumy, P. *J. Org. Chem.* **2004**, *69*, 8144.
8. Fixler, N.; Demeunynck, M.; Brochier, M.-C.; Garcia, J.; Lhomme, J. *Magn. Reson. Chem.* **1997**, *35*, 697.

9. Lown, J. W. *Chem. Soc. Rev* **1993**, *22*, 165.
10. Zhang, G.; Shen, J.; Cheng, H.; Zhu, L.; Fang, L.; Luo, S.; Mulller, M. T.; Lee, G. E.; Wei, L.; Du, Y.; Sun, D.; Wang, P. G. *J. Med. Chem.* **2005**, *48*, 2600.
11. Li, L. H.; Krueger, W. C. *Pharmacol. Ther.* **1991**, *51*, 239.
12. Renaudet, O.; Dumy, P. *Tetrahedron Lett.* **2001**, *42*, 7575.